LIMNOLOGY and OCEANOGRAPHY

ASLO

Limnol. Oceanogr. 69, 2024, 548–561

doi: 10.1002/lno.12508

Blue carbon additionality: New insights from the radiocarbon content of saltmarsh soils and their respired CO_2

Alex Houston [1*] **Mark H Garnett** [2] **William E. N. Austin** [1,3]

[1]School of Geography and Sustainable Development, University of St Andrews, St Andrews, UK
[2]National Environmental Isotope Facility, Scottish Universities Environmental Research Centre, East Kilbride, UK
[3]Scottish Association for Marine Science, Dunstaffnage, United Kingdom

Abstract

International policy frameworks recognize the net drawdown and storage of atmospheric greenhouse gases through management interventions on blue carbon ecosystems (saltmarshes, mangroves, seagrasses) as potential emissions offset strategies. However, key questions remain around the "additionality" of the carbon sequestered by these ecosystems, and whether some fraction of the organic carbon (OC) that does not derive from in situ production (allochthonous) should be included in carbon budgets. This study compares the radiocarbon (^{14}C) contents of saltmarsh soils and CO_2 evolved from aerobic laboratory incubations to show that young OC is preferentially respired over aged OC, and that the latter is also vulnerable to remineralization under oxic conditions. This highlights that management interventions which reduce the exposure of saltmarsh soils to oxic conditions support the inclusion of some portion of allochthonous OC in carbon budgets. Elevated temperature incubations provide preliminary evidence that the predominant source of respired OC will not change under predicted future warmer conditions. Saltmarsh typology also influences the ^{14}C content of both the bulk soil and respired CO_2, highlighting the importance of site selection for optimized blue carbon additionality.

Blue carbon ecosystems (BCEs), such as saltmarshes, accumulate organic carbon (OC) over millennia (Mcleod et al. 2011; Macreadie et al. 2021; Friess et al. 2022) and store vast amounts of carbon (> 30,000 Tg). There is significant public and private interest in using these systems for their potential climate mitigation and adaptation benefits, through management interventions including habitat protection, restoration, and creation (Needelman et al. 2018; Macreadie et al. 2019; Friess et al. 2022).

The protection and restoration of BCEs could deliver an offset of up to 3% of global emissions annually and is estimated to have a potential worth > $10 billion from private markets alone (Friess et al. 2022). In fact, voluntary carbon markets have facilitated the initiation of successful blue carbon projects for climate mitigation (Needelman et al. 2018; Friess et al. 2022). Verified Carbon Standard (VCS; VERRA 2021) projects are initiated for climate regulation, however projects initiated for purposes such as biodiversity gain have earlier achieved successful climate mitigation (McMahon et al. 2023). These initiatives have coincided with a rapidly evolving evidence base to quantify and understand BCEs, and in 2019, Macreadie et al. (2019) identified 10 key outstanding blue carbon research questions. One of these priority questions concerned the need to empirically understand the sources of carbon accumulating in BCEs.

Saltmarshes sequester OC produced through aboveground and belowground plant production (autochthonous sources), while also accumulating terrestrial and marine sediments deposited during tidal inundation (allochthonous sources) (Komada et al. 2022). The proportion of these OC source contributions are highly variable, with some saltmarshes dominated by autochthonous inputs (typically organogenic soils), while others accumulate varying amounts of allochthonous OC (often as minerogenic soils) (Komada et al. 2022).

The source of the OC in saltmarsh soils is important as it plays a role in how much of the total OC accumulating in these ecosystems can be attributed to direct sequestration of carbon from the atmosphere, in turn aiding climate mitigation through the reduction in the amount of atmospheric greenhouse gases (GHGs) (Macreadie et al. 2019; VERRA 2023). Only

*Correspondence: ah383@st-andrews.ac.uk

Additional Supporting Information may be found in the online version of this article.

Author Contribution Statement: A.H. undertook the study, fieldwork, sample processing, data acquisition, and wrote the first draft of the manuscript. A.H., W.A., and M.G. contributed to designing the study, fieldwork, and laboratory analyses. W.A. and M.G. oversaw the study and contributed to writing the manuscript.

under appropriate management conditions (i.e., restoring or protecting a BCE), is this process termed "additionality" (IPCC 2014; VERRA 2023). However, some authors have suggested that the trapping of a portion of the allochthonous OC in saltmarsh soils cannot be directly attributed to the reduction of atmospheric CO_2 concentrations because that carbon was originally sequestered elsewhere in the environment and subsequently transported to the saltmarsh (Needelman et al. 2018; Gallagher et al. 2022).

According to guidelines from the voluntary emissions offsets company VERRA, a portion of the allochthonous OC—that portion which is bound to mineral surfaces—must be deducted from total OC for minerogenic saltmarsh carbon crediting projects unless it can be proven that in the absence of the project (i.e., the management intervention) the allochthonous OC would have been lost to the atmosphere through remineralization (i.e., that the management intervention of the project delivers avoided emissions through the long-term burial of allochthonous OC at the site) (Needelman et al. 2018; VERRA 2023). The Intergovernmental Panel on Climate Change (IPCC) guidelines, which Governments may adopt for implementation of saltmarsh GHG emission accounting as part of their Nationally Determined Contributions (i.e., the inclusion of BCEs in their GHG emissions budgets to reach net-zero), do not require a deduction for allochthonous OC (IPCC 2014; Lovelock et al. 2022). These divergent approaches for dealing with additionality (and hence the significance of OC sources in saltmarsh soils) highlight the need for further research to understand how allochthonous and autochthonous OC components are stored and/or remineralized from saltmarsh ecosystems, with implications for improved blue carbon accounting.

As well as accumulating OC, saltmarshes also respire CO_2 aerobically from oxygenated portions of the soil profile, for example, during periods of exposure during low tide as the water table deepens (McTigue et al. 2021). Additional mechanisms of OC loss co-occur with this aerobic respiration of the soil OC pool; these include anaerobic CH_4 and CO_2 respiration and lateral fluxes of dissolved carbon species (Al-Haj and Fulweiler 2020; Santos et al. 2021), but these are not considered further here.

To further complicate matters, it is increasingly recognized that there may be variable reactivity and turnover times of these different OC sources (Leorri et al. 2018; Van de Broek et al. 2018; Komada et al. 2022). The in situ (autochthonous) sources of OC in saltmarsh soils are fresh organic matter (OM), made up of (mostly) labile OM compounds; these therefore tend to be readily available for respiration by microbial communities (McTigue et al. 2021; Komada et al. 2022; Smeaton and Austin 2022). The imported OM (allochthonous) components have been found to have a greater proportion of compounds which are resistant to respiration, either being more recalcitrant or protected through mineral association (Van de Broek et al. 2018; Mueller et al. 2019; Komada et al. 2022). Komada et al. (2022) found that carbon burial and CO_2 emissions were decoupled in a minerogenic saltmarsh in California, USA, due to the rapid turnover of contemporary autochthonous OC and long-term storage of stable, preaged allochthonous OC. Van de Broek et al. (2018) reached similar conclusions for minerogenic, estuarine saltmarshes in the Scheldt Estuary (Belgium and the Netherlands), as did Mueller et al. (2019) for saltmarshes in the European Wadden Sea.

Although autochthonous OM is viewed as mostly labile and vulnerable to mineralization under aerobic conditions, a relatively smaller proportion of allochthonous OM is also labile under aerobic conditions (Middelburg et al. 1997; Van de Broek et al. 2018).

The previous work determining the difference in carbon turnover rates between autochthonous and allochthonous sources of carbon have employed indirect methods, mainly density separation on distinct soil depth increments followed by ^{14}C and ^{13}C measurement of the different fractions which represent autochthonous and allochthonous OC (Van de Broek et al. 2018; Komada et al. 2022). Using variation with depth to infer changes with time assumes a constant input term and this oversimplification is potentially complicated by temporal changes in the proportion of OC sources accumulating at the sediment surface as the saltmarsh evolves (Van de Broek et al. 2018). Root productivity can inject young OM into soils as deep as 40 cm, which can also complicate a depth-for-time approach (Bernal et al. 2017).

Sediment traps have been used to quantify the difference in OM properties between the contemporary allochthonous sediment deposited on these traps and the bulk soil (Van de Broek et al. 2018). However, this method may be impacted by redeposition of eroded soils from within the saltmarsh site, contributing autochthonous OM to the material captured in the sediment trap (Luk et al. 2021). Other methods to quantify the sources of OC accumulating in saltmarshes have been attempted, for example with bulk and compound-specific stable isotopes, but these have been limited in their success due to overlapping signatures of sources, complexity, and cost (Geraldi et al. 2019).

^{14}C dating provides an estimate of when the OM was isolated from the atmosphere (Hajdas et al. 2021; Komada et al. 2022). In the 1950's, atmospheric nuclear weapons testing caused a spike in atmospheric ^{14}C, causing carbon sequestered after 1955 to have a %Modern ^{14}C of > 100, often referred to as "post-bomb" (Hajdas et al. 2021). The ^{14}C CO_2 concentration in 2022 was ca. 99.7 %Modern, as atmospheric concentrations have steadily decreased since a peak in ca. 1963 (Hajdas et al. 2021; Hua et al. 2022). Therefore, a "pre-bomb" ^{14}C concentration (< 100 %Modern) could also be very recent. Bulk soil samples from minerogenic saltmarshes likely contain multiple OM sources of varying ages, and eroded soils from within the marsh site may be re-deposited on the marsh surface, so while ^{14}C cannot be used to trace the precise OM source, this 100 %Modern marker can be used to assign a predominantly young (post-1955), or predominantly aged source for surficial soil samples (Komada et al. 2022).

We propose a method for qualitatively determining the differential turnover rates of saltmarsh carbon by measuring the radiocarbon (^{14}C) content of both the bulk soil and respired CO_2 from aerobic laboratory incubations. The ^{14}C content of respired CO_2 has previously been measured from terrestrial ecosystems such as peatlands (Hardie et al. 2005; Briones et al. 2010; Garnett et al. 2019), but has yet to be applied to saltmarsh soils at the time of manuscript submission. Here, we use ^{14}C measurements of bulk soil and respired CO_2 from temperature-controlled, aerobic laboratory incubations to investigate the turnover of saltmarsh carbon in conditions which represent a potential degradation scenario (e.g., drainage), and to determine the effects of elevated temperature on the source of CO_2 emissions. We hypothesized that young OC would be preferentially respired over aged OC, and that more of the aged OC would be respired from the elevated temperature incubation.

Methods

Field sites

Three contrasting saltmarshes in Scotland were sampled: Kyle of Tongue (KoT), Loch Laich (LL), and Skinflats (SK) (Fig. 1). KoT and LL are loch-head saltmarshes (Fig. 1), which are found in sheltered areas of sea-lochs (fjords) and are the prevalent saltmarsh typology along the North (KoT) and West (LL) coasts of Scotland (Haynes 2016). KoT differs from LL as the fjord it is situated in has been infilled by sediments, in addition to having a large peatland catchment (Smeaton et al. 2020). SK is an estuarine saltmarsh in Central Scotland (Fig. 1) with a high sediment supply (Clarke and Elliott 1998). SK is situated in a region of intensive land use, including landscape degradation and reclamation for agriculture, and historic coal mining (Hansom and McGlashan 2004). The sites were chosen based on existing radioisotope data from the C-SIDE project (https://www.c-side.org/) which shows that each of the sampled marshes are accreting (Miller et al. 2023, Smeaton et al., 2022). Supporting Information Table S1 summarizes key soil properties not included in the main text.

Field methods

Between June 2022 and August 2022, three replicate soil cores were taken from the low marsh of each site, ca. 30 m apart; the replication allows for an assessment of the natural variability. The low-marsh is defined by vegetation assemblage and elevation, and in this study the samples were taken towards the sea-ward edge of the low marsh (Haynes 2016;

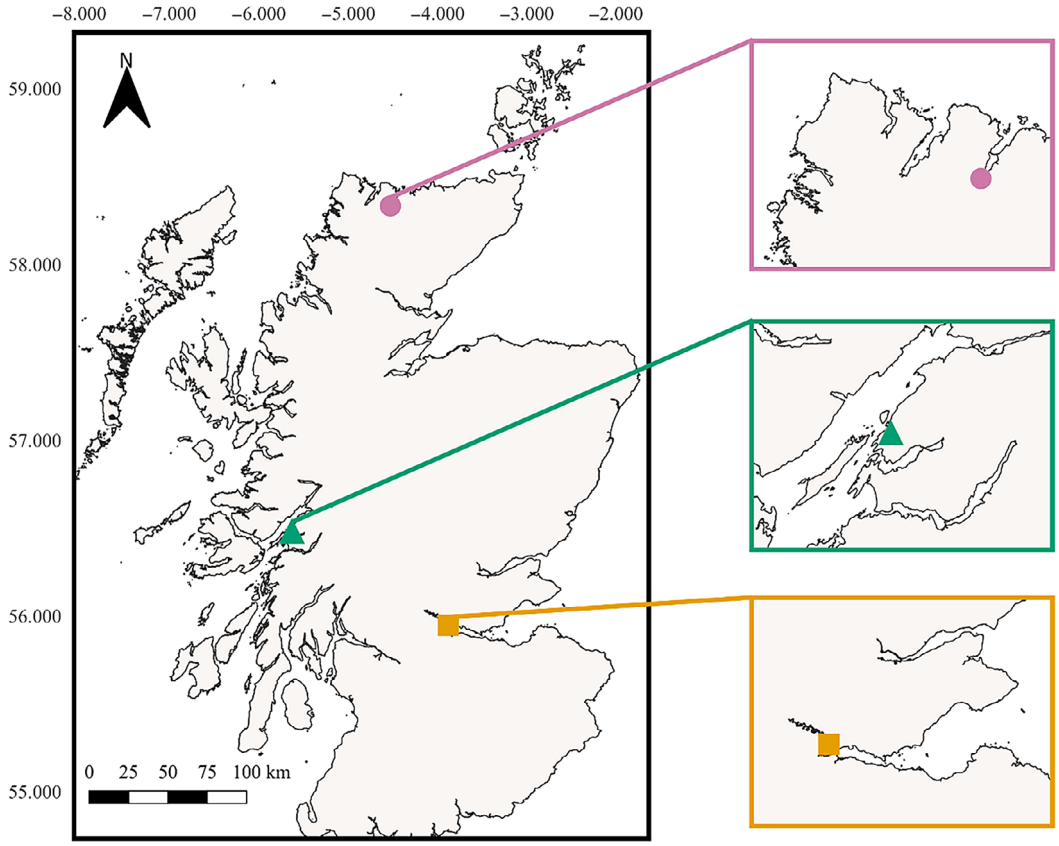

Fig. 1. Field sites denoted with markers on a map of Scotland. Inset maps to the right show zoomed in area surrounding each site: KoT (pink circle); LL (green triangle); SK (orange square).

Austin et al. 2021). A wide-diameter (10 cm) golf-hole cutter, designed to collect substantial amounts of soil material with minimal compaction was employed to recover intact cores. The core material was wrapped in foil, kept cool and returned to the laboratory within 24 h of collection and stored in a cool (4°C), dark environment to minimize OM loss prior to preparation for analysis.

Laboratory methods

Sub-sampling

Immediately upon return from the field, using a serrated knife, a full slice at 0–1, 5–6, and 19–20 cm (or the basal 1 cm if shallower) was removed from each core. The outer edge of the samples was removed to exclude potential contamination through downcore smearing, and aboveground vegetation was removed from the 0 to 1 cm samples. Each section of core was split into sub-samples for bulk ^{14}C analyses, and for the incubations. The incubation samples were stored in a refrigerated, dark room (ca. 4°C) overnight. The bulk soil ^{14}C samples were submitted to the National Environmental Isotope Facility (NEIF) Radiocarbon Laboratory for further preparation and ^{14}C measurement.

Preparation of incubation vessels

Each incubation sample was placed into a pre-weighed, airtight incubation chamber and sealed, before weighing to calculate wet sample mass. An EGM-5 infrared gas analyzer (PPSystems, USA) was connected to the gas ports of the chambers and a soda-lime cartridge to set up a closed loop of chamber—EGM-5 (gas in)—EGM-5 (gas out)—soda-lime cartridge—chamber. Chamber air was circulated through this closed loop to scrub the chamber CO_2 concentration to ca. 400 ppm (approximately current atmospheric conditions). The chambers were then placed into the appropriate incubator. One incubator was set to 11 ± 1°C to represent ambient conditions (mean maximum monthly air temperature in Scotland 1991–2020; Met Office 2023), and the other to 20 ± 1°C to represent future elevated temperature scenarios.

CO_2 concentration measurement

Within 4 h of the incubation starting, a chamber from the incubator was removed (starting with first sample placed in incubator). A closed loop of chamber—EGM-5 (gas in)—EGM-5 (gas out)—chamber was set up (Supporting Information Fig. S1), allowing CO_2 concentration to steady, before recording the concentration and time. The chamber was placed back in the incubator. This process was repeated for each chamber so that three measurements were recorded for each over 36 h. The above scrubbing and measuring procedures were repeated twice more to generate nine CO_2 concentration measurements per sample.

CO_2 collection

After the outlined CO_2 measurement procedure, samples of respired CO_2 for ^{14}C analysis were collected using the NEIF Radiocarbon Laboratory molecular sieve traps and established methods that have been shown to be reliable (Garnett et al. 2021). First, each chamber was scrubbed using soda lime to remove atmospheric CO_2. This was done in a closed loop of chamber—EGM-5 (gas in)—EGM-5 (gas out)—soda-lime trap—chamber for 10 min at a flow rate of 500 mL min^{-1} to flush the volume of the 1 liter chamber 5 times. The chambers were then returned to the incubators to respire. Chamber CO_2 concentration was monitored using the EGM-5 in a closed loop (with the gas lines scrubbed of CO_2 prior to connecting to avoid contamination) and used to establish when sufficient sample had accumulated for analysis (>3 mL CO_2, >3000 ppm). When sufficient CO_2 had accumulated it was collected for ^{14}C analysis by circulating the chamber gas through a molecular sieve cartridge using the EGM-5 pump. The chambers were placed back in the incubator. The CO_2 ^{14}C samples were submitted to the NEIF Radiocarbon Laboratory for further preparation and ^{14}C measurement.

Bulk soil and respired CO_2 ^{14}C measurement

Each bulk soil sample was rinsed with 1 M HCl to remove carbonates before rinsing with deionized water to remove mineral acid. However, prior to the incubations it was decided not to treat the incubated soils with acid as this may alter respiration processes, thus making the evolved CO_2 less representative of field conditions. Therefore, the incubated soils may have contained some carbonate which could be released as CO_2 under certain conditions (Ramnarine et al. 2012; Hajdas et al. 2021). Following the acid treatment, the bulk soil samples were dried and homogenized before cryogenically recovering the carbon as CO_2 after combusting the sample at 900°C with Copper oxide (CuO) in a sealed quartz tube. The total CO_2 trapped on the molecular sieve from the laboratory incubations was recovered by heating while purging with high-purity nitrogen gas (Research Grade 99.9995% purity, BOC, UK; Garnett et al. 2019). The CO_2 from both the bulk soil samples and the laboratory incubations was subsequently graphitised by Fe/Zn reduction and transferred to the Scottish Universities Environmental Research Centre Accelerator Mass Spectrometer (AMS) Laboratory for ^{14}C analysis. $\delta^{13}C$ (relative to Vienna PDB standard) was measured using isotope ratio mass spectrometry on a Delta V (Thermo, Germany) and used to normalize the ^{14}C results to a $\delta^{13}C = -25‰$, which were reported as %Modern ^{14}C (i.e., Fraction modern × 100).

Statistical analyses

For the bulk soil and respired CO_2 for each site, the mean ^{14}C content of the three replicate samples from the three depths was calculated, with the errors reported to one standard deviation (SD). Statistical analyses were carried out in SigmaPlot v12.5.

Results

Incubation CO_2 efflux rates

The rate of CO_2 efflux from the samples from each site decreased significantly with depth for both incubations (Kruskal–Wallis, $p < 0.05$ for both incubations; Fig. 2; Supporting Information Tables S1, S2). At each depth CO_2 efflux rates were greater from the elevated temperature incubation, but this difference was not statistically significant (Shapiro–Wilk, $p > 0.05$).

The CO_2 efflux rates from each site were tested with an ANOVA which determined that CO_2 fluxes were not significantly different between any of the sites for either the ambient or elevated temperature incubations (Kruskal–Wallis, $p > 0.05$; Kruskal–Wallis, $p > 0.05$, respectively).

Bulk soil and CO_2 ^{14}C content

The surficial soil (0.5 cm depth) %Modern ^{14}C contents for each site are < 100 %Modern, and not significantly different between KoT and LL (*t*-test; $p > 0.05$; Fig. 3A; Table 1). SK is significantly depleted in ^{14}C relative to KoT and LL (*t*-tests; $p < 0.001$ for both; Fig. 3A; Table 1). There is also greater variation in the surficial ^{14}C results at SK.

The mid-depth (5.5 cm) soil ^{14}C results are significantly enriched relative to the 0.5 cm depth samples for LL (*t*-test; $p < 0.05$; Fig. 3A) but not significantly for KoT (*t*-test, $p > 0.05$). At SK, the 5.5 cm depth ^{14}C results are slightly enriched relative to 0.5 cm depth (*t*-test, $p > 0.05$) but remain significantly depleted relative to KoT (*t*-test, $p < 0.001$) and LL (*t*-test, $p < 0.001$).

The 15.5 cm depth soil ^{14}C content is slightly depleted relative to the 5.5 cm samples for KoT (*t*-test, $p > 0.05$), with the same trend for the LL 12.5 cm depth increment relative to 5.5 cm depth (*t*-test, $p > 0.05$), but there is greater variation at this depth increment for both sites (Fig. 3A). The 17.5 cm depth ^{14}C content at SK is slightly enriched relative to the 5.5 cm depth (*t*-test, $p > 0.05$), but very depleted relative to 15.5 cm at KoT (*t*-test, $p < 0.001$) and 12.5 cm at LL (*t*-test, $p < 0.001$; Fig. 3A).

The soil ^{14}C contents for each site highlight the similarity of the soils at KoT and LL, and the depleted ^{14}C content of SK (Table 1; Fig. 3A). The bulk soil ^{14}C contents of KoT and LL are not significantly different (*t*-test, $p > 0.05$); whereas SK has significantly depleted ^{14}C content relative to both sites (ANOVA, $p < 0.001$; Fig. 3A; Table 1).

For KoT and LL, the mean CO_2 ^{14}C contents respired from the ambient incubation were > 100 %Modern for each depth increment (Table 2; Fig. 3B). Similar trends to the bulk soil ^{14}C content were evident for both sites with a slight enrichment of the 5.5 cm sample compared to the 0.5 cm depth sample for KoT (*t*-test, $p > 0.05$), and a significant enrichment of the 5.5 cm sample compared to the 0.5 cm depth sample for LL (*t*-test, $p < 0.05$). At both sites the basal (15.5 and 12.5 cm, respectively) samples display greater variation in ^{14}C content

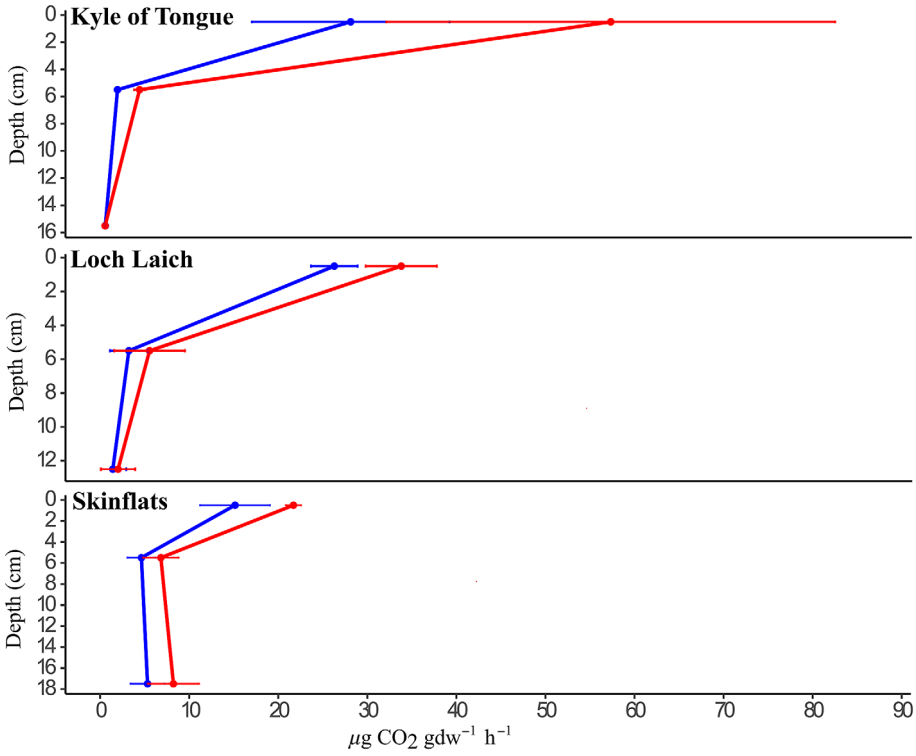

Fig. 2. Mean CO_2 fluxes per gram of dry weight (μg CO_2 gdw^{-1} h^{-1}) from the ambient (blue) and elevated temperature incubations (red) of KoT, LL, and SK. Errors are reported to one standard deviation from the mean.

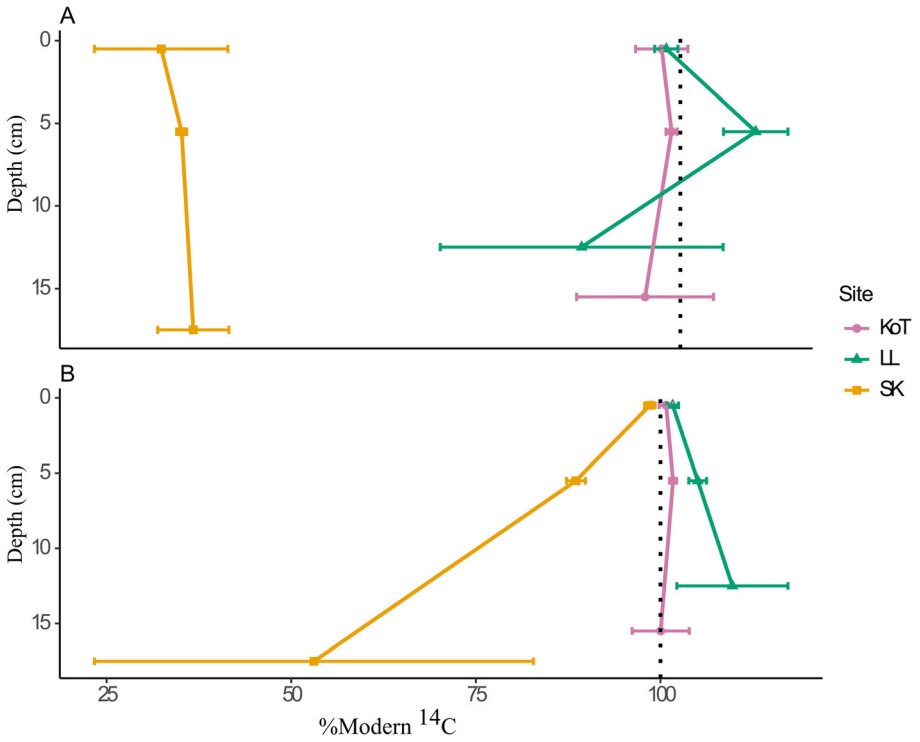

Fig. 3. Mean %Modern ^{14}C content of the (A) bulk soil and (B) respired CO_2 from the ambient temperature (11 ± 1°C) incubations of KoT, LL, SK. Vertical dotted line represents 100 %Modern ^{14}C. Errors reported to one standard deviation from the mean (Table 1).

(Table 2; Fig. 3B). All individual samples bar two from KoT were > 100 %Modern (Table 2). The mean CO_2 ^{14}C contents for the SK samples were each <100 %Modern, and significantly depleted relative to KoT (*t*-test, $p = 0.001$) and LL (*t*-test, $p < 0.05$; Table 2; Fig. 3B).

Bulk soil and respired CO_2 (ambient temperature) ^{14}C comparison

Figure 4 plots the difference ($\Delta^{14}C$; Eq. 1) between the ^{14}C content of respired CO_2 and soil, against the ^{14}C content of the soil, and shows that at ambient temperatures the CO_2 is significantly ^{14}C-enriched relative to the bulk soil (*t*-test, $p < 0.05$). This offset increases with soil ^{14}C content depletion, with a significant linear regression highlighted in Fig. 4 ($p < 0.001$). In contrast to the mostly <100 %Modern ^{14}C content of the bulk soil (Table 1), the ^{14}C content of the respired CO_2 from KoT and LL is mostly >100 %Modern, aside from two <100 %Modern samples from KoT (Table 2). Despite being significantly enriched in ^{14}C relative to the bulk soil (Fig. 4), the SK CO_2 samples have <100 %Modern ^{14}C signatures,

Table 1. Bulk soil %Modern ^{14}C content. Mean calculated to one standard deviation (SD) error as shown in Fig. 3A. The ^{13}C contents reported alongside these results are shown in Table S2.

		^{14}C content (%Modern ± 1 σ)			
Site	Depth	T1	T2	T3	Mean %Modern ± SD
KoT	0.5	99.91 ± 0.46	95.29 ± 0.42	95.29 ± 0.42	96.83 ± 2.18
KoT	5.5	99.11 ± 0.45	99.73 ± 0.46	98.22 ± 0.46	99.02 ± 0.62
KoT	15.5	91.21 ± 0.40	90.11 ± 0.40	106.85 ± 0.50	96.06 ± 7.65
LL	0.5	96.64 ± 0.45	99.68 ± 0.44	98.96 ± 0.46	98.43 ± 1.30
LL	5.5	104.82 ± 0.47	101.05 ± 0.46	112.02 ± 0.52	105.97 ± 4.55
LL	12.5	66.74 ± 0.29	101.96 ± 0.44	98.22 ± 0.46	88.97 ± 15.80
SK	0.5	47.49 ± 0.23	31.47 ± 0.15	47.03 ± 0.22	42.00 ± 7.44
SK	5.5	45.03 ± 0.20	43.69 ± 0.21	44.15 ± 0.21	44.29 ± 0.56
SK	17.5	41.36 ± 0.19	50.93 ± 0.24	44.48 ± 0.21	45.59 ± 3.99

Table 2. %Modern ^{14}C content of the respired CO_2 from the ambient temperature (11 ± 1°C) incubations of KoT, LL, SK. Mean calculated to one standard deviation (σ) error as shown in Fig. 3B. The ^{13}C contents reported alongside these results are shown in Table S3.

		^{14}C content (%Modern ± 1 σ)			
Site	Depth	T1	T2	T3	Mean %Modern ± SD
KoT	0.5	100.57 ± 0.46	99.73 ± 0.46	102.03 ± 0.47	100.78 ± 0.95
KoT	5.5	101.03 ± 0.47	102.07 ± 0.44	102.01 ± 0.45	101.70 ± 0.48
KoT	15.5	94.89 ± 0.44	104.23 ± 0.48	100.97 ± 0.46	100.03 ± 3.87
LL	0.5	100.66 ± 0.46	101.75 ± 0.44	102.58 ± 0.45	101.66 ± 0.79
LL	5.5	106.25 ± 0.46	104.34 ± 0.48	103.84 ± 0.48	104.81 ± 1.04
LL	12.5	120.12 ± 0.52	106.58 ± 0.47	102.53 ± 0.47	109.75 ± 7.52
SK	0.5	99.15 ± 0.45	98.97 ± 0.43	97.56 ± 0.43	98.56 ± 0.71
SK	5.5	87.18 ± 0.38	90.26 ± 0.40	88.22 ± 0.41	88.56 ± 1.28
SK	17.5	36.13 ± 0.36	94.86 ± 0.44	28.25 ± 0.37	53.08 ± 29.72

with two outliers which have extremely depleted ^{14}C contents (Table 2).

$$\Delta^{14}C = {}^{14}CO_2 - {}^{14}C_{soil}. \quad (1)$$

Respired CO_2 comparison of ambient and elevated temperature ^{14}C content

The ^{14}C content of the CO_2 evolved from elevated temperature (20 ± 1°C) incubations of sub-samples from the three cores from each site for the 5.5 cm depth increment were also measured and compared to the ^{14}C content of the CO_2 evolved from ambient temperature (11 ± 1°C) incubations (Fig. 5; Eq. 2). Figure 5 shows that there is no significant difference in the ^{14}C content between the temperature treatments (*t*-test, $p > 0.05$; Tables 2, 3; Fig. 5). In general, the ^{14}C samples from the elevated temperature incubation were slightly ^{14}C depleted relative to the ambient temperature incubation, with one outlier from SK (−22.57 %Modern ^{14}C difference). This outlier was caused by significant depletion of the elevated

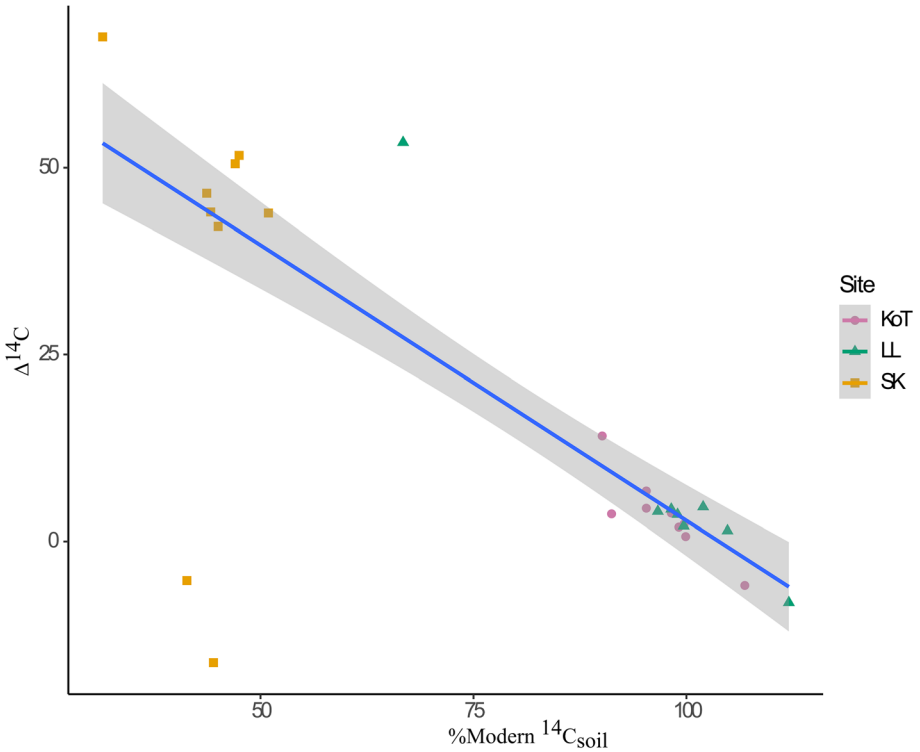

Fig. 4. ^{14}C offset ($\Delta^{14}C$) between bulk soil and respired CO_2 from ambient (11 ± 1°C) incubations of samples from KoT, LL, SK. $\Delta^{14}C$ is the difference between $^{14}CO_2$ and $^{14}C_{soil}$ (Eq. 1) and ^{14}C content is reported as %Modern. Positive values correspond to enrichment of $^{14}CO_2$ relative to $^{14}C_{soil}$. Linear regression (blue line) with 95% confidence interval (gray shading) highlights the relationship between ^{14}C offset and bulk soil ^{14}C content ($\Delta^{14}C = 65.824 - [0.629 * {}^{14}C_{soil}]$). The regression excludes the two SK outliers to the bottom left of the figure.

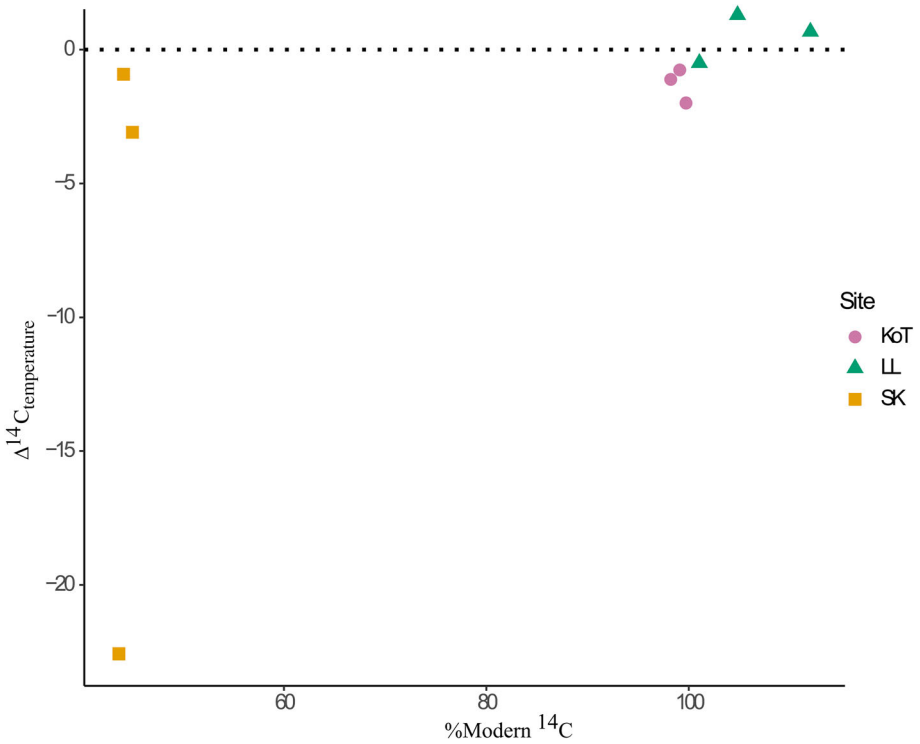

Fig. 5. ^{14}C offset between the respired CO_2 from ambient (11 ± 1°C) and elevated (20 ± 1°C) incubations of samples from KoT, LL, SK. The horizontal dotted line represents 0 %Modern $\Delta^{14}C_{temperature}$. $\Delta^{14}C_{temperature}$ (Eq. 2) is the difference between $^{14}CO_{2\ elevated}$ and $^{14}CO_{2\ ambient}$ and ^{14}C content is reported as %Modern. Negative values correspond to depletion of the ^{14}C respired at the elevated temperature relative to the ambient temperature incubation ^{14}C.

temperature sample relative to the sample from the ambient temperature incubation for SK T2 17.5 cm (Tables 2, 3). If this outlier is excluded from the dataset, the difference between the ^{14}C content of the CO_2 respired from the two temperature treatments remains insignificant (*t*-test, $p > 0.05$).

Discussion

Intersite differences in soil ^{14}C content

The surficial soil (0.5 cm depth) ^{14}C results for each site in this study are < 100 %Modern (Fig. 3A). It is not possible to state whether the 0.5 cm depth soil samples at KoT T1 and LL T2 are predominantly post- or pre- bomb, as they have ^{14}C signatures > 99.7 %Modern (current atmospheric concentration) but < 100 %Modern (Table 1). The remaining 0.5 cm depth soil samples from KoT and LL have pre-bomb ^{14}C contents which are < 99.7 %Modern, indicating that they contain an aged OC component (Hajdas et al. 2021). This component appears to have a much stronger signal at SK, as the ^{14}C is considerably depleted (Fig. 3A). The greater variation in the 0.5 cm depth ^{14}C results at SK than KoT and LL is indicative of a range of sources of varying ages accumulating in the soil, typical of the estuarine setting of SK (Leorri et al. 2018; Miller et al. 2023). The relative ^{14}C enrichment of the mid-depth (5.5 cm) soil compared to 0.5 cm depth at each site (Fig. 3A) may have been caused by the ca. 1963 ^{14}C bomb spike rapidly elevating atmospheric ^{14}C amounts to >100 %Modern (post-bomb) concentrations which have steadily decreased since (Hajdas et al. 2021; Hua et al. 2022) and are consistent with the published radioisotope stratigraphy which demonstrate high OC accumulation rates at SK

Table 3. ^{14}C content of the respired CO_2 from the elevated temperature (20 ± 1°C) incubations of KoT, LL, SK (%Modern ± 1 σ). The ^{13}C results reported alongside these results are shown in Supporting Information Table S4.

		^{14}C content (%Modern ± 1 σ)			Mean
Site	Depth	T1	T2	T3	%Modern ± SD
KoT	5.5	100.27 ± 0.44	100.08 ± 0.46	100.89 ± 0.46	100.41 ± 0.35
LL	5.5	107.55 ± 0.49	103.84 ± 0.45	104.51 ± 0.48	105.30 ± 1.61
SK	5.5	84.10 ± 0.40	67.69 ± 0.35	87.30 ± 0.41	79.70 ± 8.59

(Miller et al. 2023). Roots can inject young OM at up to 40 cm depth, which could contribute OM of varying ages to the 5.5 cm depth increments, potentially adding ^{14}C-enriched OM at this depth (Bernal et al. 2017). Importantly, post-bomb ^{14}C could be autochthonous OM or young, allochthonous OM from the local catchment or adjacent marine environment. In this study, we are not able to differentiate between young, allochthonous OM and young, autochthonous OM due to overlapping ^{13}C signatures of end-member sources (Smeaton and Austin 2017). The relative ^{14}C depletion of the basal soil samples at KoT and LL (15.5 and 12.5 cm, respectively) compared to 5.5 and 0.5 cm (Fig. 3A) is likely driven by the OM at these depths being isolated from the atmosphere prior to the ^{14}C bomb-spike (Hajdas et al. 2021) and/or the disproportionate contribution of aged, refractory OM to the long-term store as young, labile OM is preferentially remineralized (Leorri et al. 2018; Van de Broek et al. 2018; Komada et al. 2022). At SK the 17.5 cm depth bulk soil ^{14}C content is slightly enriched relative to the 5.5 and 0.5 cm depth soil samples (Fig. 3A). Published radioisotope stratigraphy for SK indicates that all soil OM in the SK samples was accumulated into the saltmarsh soil post-bomb ^{14}C spike, which may explain this slight enrichment at depth (Miller et al. 2023). As with the 5.5 cm depth increment, the injection of young OM by root productivity is possible, which could enrich the ^{14}C content of the deepest samples from each site as all are <20 cm deep (Bernal et al. 2017).

The mean bulk soil ^{14}C contents (Fig. 3A) highlight the similarity of the soils at KoT and LL, and the depleted ^{14}C content of SK. This may be related to saltmarsh typology, as KoT and LL are loch-head (fjord) saltmarshes, whereas SK is a saltmarsh fringing a sediment rich estuary (Clarke and Elliott 1998; Haynes 2016) (Fig. 1). Leorri et al. (2018) showed that the age and reactivity of saltmarsh soil OM varies with saltmarsh typology, and catchment geomorphology. At SK, there may be fossil/petrogenic contamination from the sedimentary rock in the catchment, historic coal mines, a nearby oil refinery at Grangemouth, and/or unloading of shipped coal at the former Longgannet power station on the opposite side of the estuary (Miller et al. 2023). Any of these OC sources would be ^{14}C dead and cause the soil ^{14}C content to be depleted. There is likely also aged allochthonous carbon transported from the catchment which has experienced extensive land use change and landscape degradation (Hansom and McGlashan 2004; Miller et al. 2023) facilitating the transport of deep soils (e.g., from drainage of peatland for agriculture) to the site where they are trapped by vegetation and accumulated into the saltmarsh soil. The ^{14}C contents were more enriched for KoT and LL than SK (Fig. 3A), suggesting that KoT and LL are more reliant on young OM inputs for building their soil carbon pools, whereas SK is more reliant on aged OM inputs. The sample ^{13}C signatures (Supporting Information Table S2) are within the range of typical organic sources accumulating in saltmarsh soils (Leng et al. 2006; Leng and Lewis 2017).

Intersite differences in CO_2 ^{14}C content respired from ambient temperature incubations

Almost all the respired CO_2 samples from KoT and LL had >100 %Modern ^{14}C contents, indicating that they were isolated from the atmosphere post-bomb (Table 2; Fig. 3B). As atmospheric ^{14}C concentrations are currently ca. 99.7 %Modern, the KoT T2 0.5 cm depth sample may either be post-or pre-bomb (Table 2). All other samples lie outside of this range (Table 2). Opposing both KoT and LL, the mean CO_2 ^{14}C contents for the SK samples at each depth increment were <100 % Modern, with no post-bomb samples (Table 2; Fig. 3B). As all autochthonous OM in the SK samples was likely isolated from the atmosphere after the bomb ^{14}C peak (Miller et al. 2023), any pre-bomb ^{14}C signatures can be assumed to be of either predominantly allochthonous origin, or redeposited autochthonous OM eroded from soils within the site.

The SK CO_2 17.5 cm depth samples had very different ^{14}C contents (94.86 %Modern, 36.13 %Modern and 28.25 %Modern). Two of these samples had extremely enriched stable carbon (^{13}C) signatures (−6.1‰ and −3.7‰) relative to all other samples (−20‰ to −27‰) (Supporting Information Table S3). As with the bulk soil samples discussed previously, there could also be ^{14}C-dead sources included in these soils such as coal or sedimentary rocks depleting these signatures. Despite petrogenic OM being regularly assumed to be resistant to remineralization (Chew and Gallagher 2018; Li et al. 2021), it was recently observed in an OM limited, high-Arctic fjord that that it can be used by microbial organisms (Ruben et al. 2023). Similarly, it has been reported that microbes can use OM from terrestrial shales, which are found in the SK catchment (Petsch et al. 2001; Miller et al. 2023). However, this does not imply that petrogenic OM is additional in terms of climate regulation. Remineralization rates of petrogenic OM are also likely to be slow, with minimal GHG emissions over the next century, despite observed remineralization in some studies (Petsch et al. 2001; Ruben et al. 2023). We dismiss petrogenic origin as the predominant source for the two extremely aged SK CO_2 samples as these sources would be expected to have ^{13}C signatures vastly depleted relative to those reported in this study (Supporting Information Table S3) (Ruben et al. 2023). Instead, we propose that these two outlying CO_2 samples were released from aged carbonates in the incubated soil (*see* Methods) which would have enriched ^{13}C signatures (Ramnarine et al. 2012; Brand et al. 2014).

Aside from these two samples, the remainder of the predominantly aged OM respired from SK have ^{13}C signatures within the typical range of OC sources reported in the literature (Supporting Information Tables S4, S5) (Leng et al. 2006; Leng and Lewis 2017). Despite a potentially inorganic source

for two of the SK samples, which we would not consider to be additional due to uncertainty of the net climate effect of inorganic carbon formation and dissolution in BCEs (Santos et al. 2021; Van Dam et al. 2021), the remaining seven are likely of organic provenance and provide evidence for the respiration of predominantly aged OM.

In low-oxygen environments such as saltmarshes, the bioavailability of OM is determined both by the lability of the OM substrate, and thermodynamic favorability of the terminal electron acceptor (Gunina and Kuzyakov 2022; Noyce et al. 2023). As oxygen is a thermodynamically favorable terminal electron acceptor, if its availability increases, previously stable OM can become vulnerable to respiration (Spivak et al. 2019; Gunina and Kuzyakov 2022; Noyce et al. 2023). This process may have caused the respiration of aged, previously stable OM from the SK incubations (Fig. 3B).

Thus, we provide evidence for the importance of saltmarsh environments as stores of aged, reactive OM which may be vulnerable to remineralization upon a change in environmental conditions. We did not compare these aerobic incubations to "in situ" conditions so our interpretations with respect to the additionality of aged OM assume that the rate of OM remineralization is lower in "in situ" conditions than in this set of aerobic incubations, which simulate a potential degradation scenario. In wetland soils, aerobic respiration of OM is a more efficient process than anaerobic respiration (Chapman et al. 2019; Spivak et al. 2019).

Respiration of young OC over aged OC

Laboratory incubations confine the potential C sources to the soil in the incubation chamber, limiting atmospheric contamination which is a risk from field-based CO_2 collection. This facilitates the direct comparison of the ^{14}C content in the bulk soil and evolved CO_2 from these incubations (Fig. 4) (Briones et al. 2010). The switch from the mostly pre-bomb ^{14}C content of the KoT and LL soils (Fig. 3A) to the mostly post-bomb ^{14}C content of the ambiently respired CO_2 (Fig. 3B) indicates that at these two sites, young OC is preferentially respired over aged OC. For KoT and LL, as the bulk soil samples are close to 100 %Modern ^{14}C and are potentially a mix of pre- and post-bomb C, with the latter varying considerably in ^{14}C content over a few decades, there could be scenarios where different aged material to the bulk soil are respired but result in no significant overall change in the ^{14}C content. Despite the SK CO_2 samples being considerably depleted in ^{14}C relative to KoT and LL (Fig. 3B), they are significantly enriched in ^{14}C relative to the bulk soil (Fig. 4). This clearly demonstrates that for this set of experiments, young OM is preferentially respired over aged OM. Despite this, the pre-bomb ^{14}C content of the respired CO_2 from SK indicates that aged OC is respired from these soils.

Published literature on carbon cycling in saltmarshes have found that young OM is remineralized at a faster rate than aged OM, and the latter contributes disproportionately to long-term storage (Leorri et al. 2018; Van de Broek et al. 2018; Komada et al. 2022). This is generally attributed to the bioavailability of different OM sources, with young OM considered to be more labile than old OM which is often allochthonous in origin and mineral associated, increasing its stability (Komada et al. 2022). Research on terrestrial soils has shown that all OM is degradable but at varying rates (Lehmann and Kleber 2015). In agreement with this literature, we show that young OM is preferentially respired over aged OM but that the latter is also vulnerable to remineralization in oxic conditions.

Verified Carbon Standard projects work on much longer timescales (decadal) than this set of incubation experiments (ca. 14–30 d). Carbon budgets should account for all GHG emissions within project timescales (VERRA 2023), and it is therefore possible that less reactive, aged OM would be increasingly respired throughout project timescales as young, more bioavailable sources become depleted (Lehmann and Kleber 2015). Thus, despite predominantly young OM being respired from KoT and LL (Fig. 3B), this does not rule out the possibility of aged OM being respired in a longer-term incubation. However, an increasing proportion of aged OM to respired GHGs does not mean that aged OM is having an increasing impact on the stability of the long-term OM pool, as respiration rates may be slower than when younger OM was the predominant source. Therefore, as the incubations were relatively short-term (ca. 14–30 d), it is unlikely that there was a complete depletion of any single OC source from these soils. Under in-situ conditions there may be temporal changes in the source of OC respired which cannot be accounted for in these experiments. For example, variable temperatures experienced by the saltmarshes in-situ conditions may cause a rate shift in the source of OC respired, and this may be exacerbated by climate change (McTigue et al. 2021). Additional factors such as the pulsing of seawater can alter OC protection mechanisms and cause a change in the source of OC respired (Spivak et al. 2019).

Potential changes in the age of OC respired at elevated temperatures

Our study aimed to determine whether the lack of significant change in CO_2 flux rates between the incubation temperature treatments (Fig. 2) corresponded to a change in the OM source respired. Due to the carbon-quality temperature (CQT) hypothesis which states that at elevated temperatures, more chemically complex OM is respired over chemically simple OM (McTigue et al. 2021), we proposed that the evolved CO_2 would be ^{14}C depleted (older) at the elevated temperature incubation relative to the ambient temperature incubation. No significant differences were found, although the CO_2 respired at the elevated temperature was generally slightly ^{14}C depleted relative to the CO_2 respired at the ambient temperature.

As the soils are potentially a mix of pre- and post-bomb C, with the latter varying substantially in ^{14}C content over a few decades, there could be scenarios where different aged material responds differently to temperature, but which results in no significant overall change in the $^{14}CO_2$. Acknowledging this limitation, as there are no significant differences observed, we conclude that elevated temperature does not cause a change in the source of the respired CO_2 from this set of incubation experiments. This is supported by no significant changes in ^{13}C content (Supporting Information Tables S4, S5). These are the first data to empirically test the potential impact of temperature on the OM source respired.

Implications of these data for blue carbon additionality

The sources of OM stored in saltmarsh soils can be variable in age and reactivity. Van de Broek et al. (2018) used soil ^{14}C fractionation to demonstrate that the long-term (centennial) OC store of a saltmarsh in Belgium was driven by pre-aged, allochthonous inputs and that autochthonous OM was remineralized over decadal timescales. These authors also demonstrated that the age of the allochthonous OM deposited on the saltmarsh surface varied seasonally with greater estuarine phytoplankton productivity in summer months causing younger allochthonous OM to be deposited on the marsh surface (Van de Broek et al. 2018). They found that the young, allochthonous OM deposited on the marsh surface during summer months was not observed downcore, indicating that the aged, allochthonous OM was driving the long-term OC store. Similarly, Komada et al. (2022) and Mueller et al. (2019) highlighted that aged, recalcitrant OM was remineralized at a slower rate than young, labile OM from minerogenic saltmarshes in California (USA), and the Wadden Sea (Germany), respectively. Both studies showed that the aged OM contributed disproportionately to the long-term OC store. While allochthonous OM can be variable in both age and reactivity, our results highlight the importance of allochthonous sources of aged OM to long-term OC storage in saltmarsh soils, with important implications for additionality.

Recently published radiometric carbon accumulation rates for SK, "date" the marsh formation to ca. 1931, so autochthonous OM isolated from the atmosphere when the marsh formed would have a pre-bomb (pre-1955) ^{14}C content (Miller et al. 2023). We assume that the cores analyzed in both this study and Miller et al. (2023) will have roughly similar sediment accumulation rates. Thus, autochthonous saltmarsh OM eroded from creekbanks and re-deposited on the marsh surface could contribute pre-bomb, autochthonous OM, as observed by Luk et al. (2021). Atmospheric ^{14}C contents in 1931 were ca. 98 %Modern (http://calib.org/CALIBomb/), which is greater than the ^{14}C content of all but two SK CO_2 samples evolved from the ambient temperature incubation (Table 2). Therefore, we infer that a portion of the CO_2 respired from SK was aged and allochthonous in origin as it was likely isolated from the atmosphere prior to the marsh forming at this site. Due to the rapid sediment accumulation rates (Miller et al. 2023) and depleted bulk soil ^{14}C content of SK (Fig. 3A), we assume that allochthonous inputs to this site are relatively high. The OM transported through estuarine systems and deposited on saltmarshes can have variable reactivity and age, which may provide an explanation as to why aged CO_2 was respired from this set of aerobic incubations (Canuel and Hardison 2016; Van de Broek et al. 2018; Huang et al. 2023). As predominantly pre-bomb CO_2 was respired from SK (estuarine saltmarsh), but predominantly post-bomb CO_2 was respired from KoT and LL (loch-head saltmarshes), it is possible that saltmarsh typology impacts the carbon cycling in these soils. It is also likely that this is caused by a greater diversity of OC sources accumulating in the SK marsh, as estuarine settings are known to transport OM of a range of ages and reactivities.

Allochthonous OM can be young (post-bomb) and labile, especially during summer months (when the cores for this study were taken) due to phytoplankton productivity (Middelburg et al. 1997; Boschker et al. 1999; Van de Broek et al. 2018). Therefore, we cannot interpret whether the post-bomb CO_2 respired from KoT and LL is predominantly autochthonous or allochthonous in origin. Instead, we infer that the source of CO_2 respired likely depends on the reactivity of the OM, and that OM reactivity decreases with age. Further research on the role of intrinsic molecular reactivity, protection mechanisms such as mineral association for the preservation of OM sources, and the effects of disturbances on OM dynamics in BCEs is required to better constrain blue carbon additionality.

SK (estuarine, high sediment supply) has rapid carbon accumulation rates relative to other saltmarshes in Scotland (Miller et al. 2023). This suggests that projects for blue carbon gains should be targeted towards estuarine saltmarshes with a high sediment supply in order to generate the greatest carbon additionality. The bulk soil ^{14}C contents presented in this study (Fig. 3A) highlight that a large proportion of the SK OC is likely pre-aged and potentially allochthonous in origin. This study did not quantify mineral association so we cannot provide insight as to whether this aged OC would be deducted under current VERRA Verified Carbon Standard guidelines (Needelman et al. 2018; VERRA 2023). Despite this, the results presented in this study also show that an inferred aged, allochthonous source of OC was remineralized from SK soils when incubated in oxic conditions (Fig. 3B) and provide evidence that management interventions that prevent this from occurring may warrant its treatment as additional carbon, in line with IPCC guidelines (IPCC 2014). Management interventions for this may include activities such as blocking drainage ditches to elevate the water table and maintain saturated, anoxic conditions (Haynes 2016). Thus, this study provides evidence for the additionality of some fraction of aged, allochthonous OM accumulating in saltmarshes.

Data availability statement

All data presented in this manuscript is available in the Supporting Information.

References

Al-Haj, A. N., and R. W. Fulweiler. 2020. A synthesis of methane emissions from shallow vegetated coastal ecosystems. Glob. Change Biol. **26**: 2988–3005. doi:10.1111/gcb.15046

Austin, W. E. N., C. Smeaton, S. Riegel, P. Ruranska, and L. Miller. 2021. Blue carbon stock in Scottish saltmarsh soils. Scott. Mar. Freshw. Sci. **12**: 37. doi:10.7489/12372-1

Bernal, B., J. P. Megonigal, and T. J. Mozdzer. 2017. An invasive wetland grass primes deep soil carbon pools. Glob. Change Biol. **23**: 2104–2116. doi:10.1111/gcb.13539

Boschker, H. T. S., J. F. C. De Brouwer, and T. E. Cappenberg. 1999. The contribution of macrophyte-derived organic matter to microbial biomass in salt-marsh sediments: Stable carbon isotope analysis of microbial biomarkers. Limnol. Oceanogr. **44**: 309–319. doi:10.4319/lo.1999.44.2.0309

Brand, W. A., T. B. Coplen, J. Vogl, M. Rosner, and T. Prohaska. 2014. Assessment of international reference materials for isotope-ratio analysis (IUPAC Technical Report). Pure Appl. Chem. **86**: 425–467. doi:10.1515/pac-2013-1023

Briones, M. J. I., M. H. Garnett, and P. Ineson. 2010. Soil biology and warming play a key role in the release of "old C" from organic soils. Soil Biol. Biochem. **42**: 960–967. doi:10.1016/j.soilbio.2010.02.013

Canuel, E. A., and A. K. Hardison. 2016. Sources, ages, and alteration of organic matter in estuaries. Ann. Rev. Mar. Sci. **8**: 409–434. doi:10.1146/annurev-marine-122414-034058

Chapman, S. K., M. A. Hayes, B. Kelly, and J. A. Langley. 2019. Exploring the oxygen sensitivity of wetland soil carbon mineralization. Biol. Lett. **15**: 20180407. doi:10.1098/rsbl.2018.0407

Chew, S. T., and J. B. Gallagher. 2018. Accounting for black carbon lowers estimates of blue carbon storage services. Sci. Rep. **8**: 2553. doi:10.1038/s41598-018-20644-2

Clarke, S., and A. J. Elliott. 1998. Modelling suspended sediment concentrations in the firth of forth. Estuar. Coast. Shelf Sci. **47**: 235–250. doi:10.1006/ecss.1998.0359

Friess, D. A., J. Howard, M. Huxham, P. I. Macreadie, and F. Ross. 2022. Capitalizing on the global financial interest in blue carbon. PLoS Clim. **1**: e0000061. doi:10.1371/journal.pclm.0000061

Gallagher, J. B., K. Zhang, and C. H. Chuan. 2022. A Re-evaluation of wetland carbon sink mitigation concepts and measurements: A diagenetic solution. Wetlands **42**: 23. doi:10.1007/s13157-022-01539-5

Garnett, M. H., J.-A. Newton, and P. L. Ascough. 2019. Advances in the radiocarbon analysis of carbon dioxide at the NERC radiocarbon facility (East Kilbride) using molecular sieve cartridges. Radiocarbon **61**: 1855–1865. doi:10.1017/RDC.2019.86

Garnett, M. H., J.-A. Newton, and T. C. Parker. 2021. A highly portable and inexpensive field sampling kit for radiocarbon analysis of carbon dioxide. Radiocarbon **63**: 1355–1368. doi:10.1017/RDC.2021.49

Geraldi, N. R., and others. 2019. Fingerprinting blue carbon: Rationale and tools to determine the source of organic carbon in marine depositional environments. Front. Mar. Sci. **6**: 263. doi:10.3389/fmars.2019.00263

Gunina, A., and Y. Kuzyakov. 2022. From energy to (soil organic) matter. Glob. Change Biol. **28**: 2169–2182. doi:10.1111/gcb.16071

Hajdas, I., and others. 2021. Radiocarbon dating. Nat. Rev. Methods Primer **1**: 1–26. doi:10.1038/s43586-021-00058-7

Hansom, J. D., and D. J. McGlashan. 2004. Scotland's coast: Understanding past and present processes for sustainable management. Scott. Geogr. J. **120**: 99–116. doi:10.1080/00369220418737195

Hardie, S. M. L., M. H. Garnett, A. E. Fallick, A. P. Rowland, and N. J. Ostle. 2005. Carbon dioxide capture using a zeolite molecular sieve sampling system for isotopic studies (^{13}C and ^{14}C) of respiration. Radiocarbon **47**: 441–451. doi:10.1017/S0033822200035220

Haynes, T. A. 2016. Scottish saltmarsh survey national report. Scottish Natural Heritage Commissioned Report No. 786. p. 204. Scottish National Heritage.

Hua, Q., and others. 2022. Atmospheric radiocarbon for the period 1950–2019. Radiocarbon **64**: 723–745. doi:10.1017/RDC.2021.95

Huang, W., H. Yang, S. He, B. Zhao, and X. Cui. 2023. Thermochemical decomposition reveals distinct variability of sedimentary organic carbon reactivity along the Yangtze River estuary-shelf continuum. Mar. Chem. **257**: 104326. doi:10.1016/j.marchem.2023.104326

IPCC. 2014. 2013 Supplement to the 2006 IPCC guidelines for national greenhouse gas inventories: Wetlands methodological guidance on lands with wet and drained soils, and constructed wetlands for wastewater treatment.

Komada, T., A. Bravo, M.-T. Brinkmann, K. Lu, L. Wong, and G. Shields. 2022. "Slow" and "fast" in blue carbon: Differential turnover of allochthonous and autochthonous organic matter in minerogenic salt marsh sediments. Limnol. Oceanogr. **67**: S133–S147. doi:10.1002/lno.12090

Lehmann, J., and M. Kleber. 2015. The contentious nature of soil organic matter. Nature **528**: 60–68. doi:10.1038/nature16069

Leng, M. J., A. L. Lamb, T. H. E. Heaton, J. D. Marshall, B. B. Wolfe, M. D. Jones, J. A. Holmes, and C. Arrowsmith. 2006. Isotopes in lake sediments, p. 147–184. *In* M. J. Leng [ed.], Isotopes in palaeoenvironmental research. Springer Netherlands.

Leng, M. J., and J. P. Lewis. 2017. C/N ratios and carbon isotope composition of organic matter in estuarine

environments, p. 213–237. *In* K. Weckström, K. M. Saunders, P. A. Gell, and C. G. Skilbeck [eds.], Applications of paleoenvironmental techniques in estuarine studies. Springer.

Leorri, E., A. R. Zimmerman, S. Mitra, R. R. Christian, F. Fatela, and D. J. Mallinson. 2018. Refractory organic matter in coastal salt marshes-effect on C sequestration calculations. Sci. Total Environ. **633**: 391–398. doi:10.1016/j.scitotenv.2018.03.120

Li, Y., C. Fu, L. Zeng, Q. Zhou, H. Zhang, C. Tu, L. Li, and Y. Luo. 2021. Black carbon contributes substantially to Allochthonous carbon storage in deltaic vegetated coastal habitats. Environ. Sci. Technol. **55**: 6495–6504. doi:10.1021/acs.est.1c00636

Lovelock, C. E., and others. 2022. An Australian blue carbon method to estimate climate change mitigation benefits of coastal wetland restoration. Restor. Ecol. **n/a**: e13739. doi:10.1111/rec.13739

Luk, S. Y., K. Todd-Brown, M. Eagle, A. P. McNichol, J. Sanderman, K. Gosselin, and A. C. Spivak. 2021. Soil organic carbon development and turnover in natural and disturbed salt marsh environments. Geophys. Res. Lett. **48**: e2020GL090287. doi:10.1029/2020GL090287

Macreadie, P. I., and others. 2019. The future of blue carbon science. Nat. Commun. **10**: 3998. doi:10.1038/s41467-019-11693-w

Macreadie, P. I., and others. 2021. Blue carbon as a natural climate solution. Nat. Rev. Earth Environ. **2**: 826–839. doi:10.1038/s43017-021-00224-1

Mcleod, E., and others. 2011. A blueprint for blue carbon: Toward an improved understanding of the role of vegetated coastal habitats in sequestering CO_2. Front. Ecol. Environ. **9**: 552–560. doi:10.1890/110004

McMahon, L., C. J. T. Ladd, A. Burden, E. Garrett, K. R. Redeker, P. Lawrence, and R. Gehrels. 2023. Maximizing blue carbon stocks through saltmarsh restoration. Front. Mar. Sci. **10**.

McTigue, N. D., Q. A. Walker, and C. A. Currin. 2021. Refining estimates of greenhouse gas emissions from salt marsh "blue carbon" erosion and decomposition. Front. Mar. Sci. **8**.

Met Office. 2023. Altnaharra SAWS (Highland) UK climate averages. Met Off.

Middelburg, J. J., J. Nieuwenhuize, R. K. Lubberts, and O. van de Plassche. 1997. Organic carbon isotope systematics of coastal marshes. Estuar. Coast. Shelf Sci. **45**: 681–687. doi:10.1006/ecss.1997.0247

Miller, L. C., C. Smeaton, H. Yang, and W. E. N. Austin. 2023. Carbon accumulation and storage across contrasting saltmarshes of Scotland. Estuar. Coast. Shelf Sci. **282**: 108223. doi:10.1016/j.ecss.2023.108223

Mueller, P., N. Ladiges, A. Jack, G. Schmiedl, L. Kutzbach, K. Jensen, and S. Nolte. 2019. Assessing the long- term carbon-sequestration potential of the semi-natural salt marshes in the European Wadden Sea. Ecosphere **10**. doi:10.1002/ecs2.2556

Needelman, B. A., I. M. Emmer, S. Emmett-Mattox, S. Crooks, J. P. Megonigal, D. Myers, M. P. J. Oreska, and K. McGlathery. 2018. The science and policy of the verified carbon standard methodology for tidal wetland and seagrass restoration. Estuar. Coasts **41**: 2159–2171. doi:10.1007/s12237-018-0429-0

Noyce, G. L., A. J. Smith, M. L. Kirwan, R. L. Rich, and J. P. Megonigal. 2023. Oxygen priming induced by elevated CO_2 reduces carbon accumulation and methane emissions in coastal wetlands. Nat. Geosci. **16**: 63–68. doi:10.1038/s41561-022-01070-6

Petsch, S. T., T. I. Eglinton, and K. J. Edwards. 2001. ^{14}C-dead living biomass: Evidence for microbial assimilation of ancient organic carbon during shale weathering. Science **292**: 1127–1131. doi:10.1126/science.1058332

Ramnarine, R., C. Wagner-Riddle, K. E. Dunfield, and R. P. Voroney. 2012. Contributions of carbonates to soil CO_2 emissions. Can. J. Soil Sci. **92**: 599–607. doi:10.4141/cjss2011-025

Ruben, M., and others. 2023. Fossil organic carbon utilization in marine Arctic fjord sediments by subsurface microorganisms. Nat. Geosci. **16**: 625–630. doi:10.1038/s41561-023-01198-z

Santos, I. R., and others. 2021. The renaissance of Odum's outwelling hypothesis in "Blue Carbon" science. Estuar. Coast. Shelf Sci. **255**: 107361. doi:10.1016/j.ecss.2021.107361

Smeaton, C., and W. E. N. Austin. 2017. Sources, sinks, and subsidies: Terrestrial carbon storage in mid-latitude fjords. J. Geophys. Res. Biogeosci. **122**: 2754–2768. doi:10.1002/2017JG003952

Smeaton, C., N. L. M. Barlow, and W. E. N. Austin. 2020. Coring and compaction: Best practice in blue carbon stock and burial estimations. Geoderma **364**: 114180. doi:10.1016/j.geoderma.2020.114180

Smeaton, C., and W. E. N. Austin. 2022. Quality not quantity: Prioritizing the management of sedimentary organic matter across continental shelf seas. Geophys. Res. Lett. **49**: e2021GL097481. doi:10.1029/2021GL097481

Spivak, A. C., J. Sanderman, J. L. Bowen, E. A. Canuel, and C. S. Hopkinson. 2019. Global-change controls on soil-carbon accumulation and loss in coastal vegetated ecosystems. Nat. Geosci. **12**: 685–692. doi:10.1038/s41561-019-0435-2

Van Dam, B. R., and others. 2021. Calcification-driven CO_2 emissions exceed "blue carbon" sequestration in a carbonate seagrass meadow. Sci. Adv. **7**: eabj1372. doi:10.1126/sciadv.abj1372

Van de Broek, M., C. Vandendriessche, D. Poppelmonde, R. Merckx, S. Temmerman, and G. Govers. 2018. Long-term organic carbon sequestration in tidal marsh sediments is dominated by old-aged allochthonous inputs in a

macrotidal estuary. Global Change Biol. **24**: 2498–2512. doi:10.1111/gcb.14089

VERRA. 2023. VM0033 methodology for tidal wetland and seagrass restoration. v2.1.

Acknowledgments

We thank the NERC SUPER DTP for funding the PhD through which this research was undertaken. We acknowledge support from the National Environmental Isotope Facility in funding the ^{14}C measurements for this study under grant NE/S011587/1 (allocation numbers 2500.0422, 2594.1022). Thanks are extended to Chloe Bates, Catriona Stewart, Joanna Houston, Marion Bove, and Megan McCall for assisting with sample collection. We thank each editor and both reviewers (one anonymous and Pat Megonigal, Smithsonian Environmental Research Centre) for their helpful comments which have undoubtedly improved this manuscript.

Conflict of Interest

We declare no conflicts of interest.

Submitted 05 August 2023
Revised 13 November 2023
Accepted 25 December 2023

Associate editor: Robinson W. Fulweiler